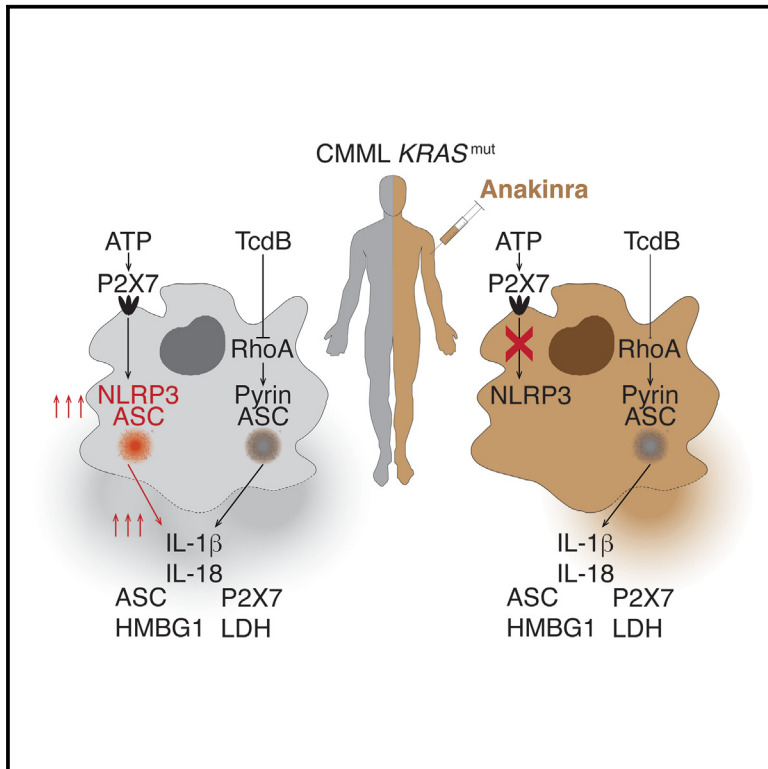


# NLRP3 inflammasome activation and symptom burden in *KRAS*-mutated CMML patients is reverted by IL-1 blocking therapy

## Graphical abstract



## Authors

Laura Hurtado-Navarro,  
 Ernesto José Cuenca-Zamora,  
 Lurdes Zamora, ..., Raúl Teruel-Montoya,  
 Pablo Pelegrín, Francisca Ferrer-Marín

## Correspondence

pablopel@um.es (P.P.),  
 fferrer@ucam.edu (F.F.-M.)

## In brief

Hurtado-Navarro et al. show that in CMML patients with *KRAS* mutation, the disease is associated with a constitutive activation of the NLRP3 inflammasome and a specific cytokine signature. Treatment with recombinant IL-1R antagonist (anakinra) resulted in clinical improvement but also an impaired activation of the NLRP3 inflammasome.

## Highlights

- CMML with *KRAS* mutation has a basal activation of NLRP3 inflammasome in monocytes
- Anakinra treatment of a *KRAS* p.G12D CMML patient impairs NLRP3 activation
- Anakinra serves as a bridge therapy to allo-HSCT in a CMML patient with *KRAS* p.G12D
- Pyrin inflammasome is not involved in CMML patients with *KRAS* mutation



## Report

# NLRP3 inflammasome activation and symptom burden in *KRAS*-mutated CMML patients is reverted by IL-1 blocking therapy

Laura Hurtado-Navarro,<sup>1,21</sup> Ernesto José Cuenca-Zamora,<sup>1,2,3,21</sup> Lurdes Zamora,<sup>4</sup> Beatriz Bellosillo,<sup>5</sup> Esperanza Such,<sup>6</sup> Eva Soler-Espejo,<sup>2</sup> Helios Martínez-Banaclocha,<sup>1,7</sup> Jesús M. Hernández-Rivas,<sup>8</sup> Javier Marco-Ayala,<sup>2</sup> Laura Martínez-Alarcón,<sup>1</sup> Lola Linares-Latorre,<sup>9</sup> Sara García-Ávila,<sup>10,11</sup> Paula Amat-Martínez,<sup>12</sup> Teresa González,<sup>8</sup> Montserrat Arnan,<sup>13</sup> Helena Pomares-Marín,<sup>13</sup> Gonzalo Carreño-Tarragona,<sup>14</sup> Tzu Hua Chen-Liang,<sup>2</sup> María T. Herranz,<sup>15</sup> Carlos García-Palenciano,<sup>1,16</sup> María Luz Morales,<sup>1,2</sup> Andrés Jerez,<sup>1,2,3</sup> María L. Lozano,<sup>1,2,3</sup> Raúl Teruel-Montoya,<sup>1,2,3,17</sup> Pablo Pelegrín,<sup>1,18,20,22,\*</sup> and Francisca Ferrer-Marín<sup>1,2,3,17,19,20,\*</sup>

<sup>1</sup>Biomedical Research Institute of Murcia (IMIB-Pascual Parrilla), Murcia, Spain

<sup>2</sup>Hematology Department, Hospital Universitario Morales-Meseguer, Centro Regional de Hemodonación, Murcia, Spain

<sup>3</sup>CIBERER CB15/00055 (U765), Murcia, Spain

<sup>4</sup>Myeloid Neoplasms Group, Josep Carreras Leukaemia Research Institute, ICO-Hospital Germans Trias I Pujol, Universitat Autònoma de Barcelona, Badalona, Spain

<sup>5</sup>Molecular Biology Laboratory, Pathology Department, Hospital Del Mar, Hospital Del Mar Medical Research Institute, IMIM, Barcelona, Spain

<sup>6</sup>Hematology Department, La Fe University Hospital, Valencia, Spain

<sup>7</sup>Immunology Service, Hospital Universitario Virgen de La Arrixaca, Murcia, Spain

<sup>8</sup>Department of Medicine, Universidad de Salamanca, Servicio de Hematología, Hospital Universitario de Salamanca, IBSAL, Salamanca, Spain

<sup>9</sup>Service of Clinical Analysis and Microbiology, Fundación Instituto Valenciano de Oncología, Valencia, Spain

<sup>10</sup>Department of Hematology, Hospital Del Mar, Barcelona, Spain

<sup>11</sup>IMIM (Hospital Del Mar Medical Research Institute), Barcelona, Spain

<sup>12</sup>Hematology Service, Clinic University Hospital, INCLIVA Health Research Institute, Valencia, Spain

<sup>13</sup>Hematology Department, Institut Català D'Oncologia (ICO)-Hospital Duran I Reynals, IDIBELL, Barcelona, Spain

<sup>14</sup>Hematology Department, Hospital Universitario 12 de Octubre, Madrid, Spain

<sup>15</sup>Internal Medicine Service, Hospital Universitario Morales Meseguer, Murcia, Spain

<sup>16</sup>Servicio de Anestesiología y Reanimación, Hospital Clínico Universitario Virgen de La Arrixaca, Murcia, Spain

<sup>17</sup>Universidad Católica San Antonio (UCAM), Murcia, Spain

<sup>18</sup>Department of Biochemistry and Molecular Biology B and Immunology, University of Murcia, Murcia, Spain

<sup>19</sup>X (formerly Twitter): @IMIB\_RMurcia

<sup>20</sup>Senior author

<sup>21</sup>These authors contributed equally

<sup>22</sup>Lead contact

\*Correspondence: [pablopel@um.es](mailto:pablopel@um.es) (P.P.), [fferrer@ucam.edu](mailto:fferrer@ucam.edu) (F.F.-M.)

<https://doi.org/10.1016/j.xcrm.2023.101329>

## SUMMARY

Chronic myelomonocytic leukemia (CMML) is frequently associated with mutations in the rat sarcoma gene (*RAS*), leading to worse prognosis. *RAS* mutations result in active *RAS*-GTP proteins, favoring myeloid cell proliferation and survival and inducing the NLRP3 inflammasome together with the apoptosis-associated speck-like protein containing a caspase recruitment domain (ASC), which promote caspase-1 activation and interleukin (IL)-1 $\beta$  release. Here, we report, in a cohort of CMML patients with mutations in *KRAS*, a constitutive activation of the NLRP3 inflammasome in monocytes, evidenced by ASC oligomerization and IL-1 $\beta$  release, as well as a specific inflammatory cytokine signature. Treatment of a CMML patient with a *KRAS*<sup>G12D</sup> mutation using the IL-1 receptor blocker anakinra inhibits NLRP3 inflammasome activation, reduces monocyte count, and improves the patient's clinical status, enabling a stem cell transplant. This reveals a basal inflammasome activation in *RAS*-mutated CMML patients and suggests potential therapeutic applications of NLRP3 and IL-1 blockers.



## INTRODUCTION

Chronic myelomonocytic leukemia (CMML) is a rare, age-related myeloid neoplasm with overlapping features of myelodysplastic syndromes and myeloproliferative neoplasms (MDSs/MPNs). It is characterized by sustained clonal monocytosis, ineffective hematopoiesis, and an inherent risk of transformation to secondary acute myeloid leukemia (sAML).<sup>1,2</sup> Cytogenetic alterations (present in only 20%–30% of patients) or molecular clonal abnormalities are supportive criteria for diagnosis.<sup>1–4</sup> Based on peripheral blood (PB) white blood cell (WBC) count, both the International Consensus Classification<sup>1</sup> and the new (5<sup>th</sup>) WHO edition of myeloid neoplasms<sup>2</sup> formally recognize two subtypes: myelodysplastic (CMML-MD) and myeloproliferative (CMML-MP), with a WBC count < or  $\geq 13 \times 10^9/L$ , respectively. Compared to the CMML-MD subtype, the CMML-MP subtype confers a worse prognosis.<sup>5–7</sup>

Importantly, CMML-MP is enriched in mutations in rat sarcoma GTPase (*RAS*) oncogenes such as *NRAS* (neuroblastoma *RAS*) and/or *KRAS* (Kirsten *RAS*).<sup>5</sup> The *RAS*/*RAF*/*MEK*/*ERK* signaling pathway regulates key cellular functions such as cell proliferation, differentiation, and survival.<sup>8</sup> It has recently been shown that *RAS* mutations not only act through its canonical signaling pathway but also contribute to malignancy through activation of NLRP3 (nucleotide-binding domain leucine-rich repeat containing with pyrin domain-containing 3).<sup>9</sup> The NLRP3 inflammasome is a multiprotein complex that is activated in response to different pathogen-associated signals and endogenous damage; its activation leads to recruitment of an adaptor protein apoptosis-associated speck-like protein containing a caspase recruitment domain (ASC), which oligomerizes to form long filaments culminating in a large intracellular oligomer called ASC “speck.” Pro-caspase-1 then binds to the oligomeric ASC filaments via homotypic interactions between the caspase recruitment domain, leading to their activation and consequently to the processing and release of the proinflammatory cytokines interleukin IL-1 $\beta$  and IL-18 via gasdermin D-dependent plasma membrane permeabilization. Gasdermin D pore formation in the plasma membrane could be repaired by recruiting the endosomal sorting complexes required for transport mechanisms and results in a living hyperactive state of the cell; however, if gasdermin D pores cannot be repaired, the cell undergoes pyroptotic cell death.<sup>10</sup>

Pyroptosis also leads to the release of ASC specks into the extracellular space, where they could amplify the inflammatory response.<sup>11–13</sup> The initial step of NLRP3 activation requires, among others, reactive oxygen species (ROS) production.<sup>14,15</sup> *KRAS* mutation leads to activation of RAC1 (Ras-related C3 botulinum toxin substrate 1) and ROS production, which favors NLRP3 inflammasome activation.<sup>9</sup> Based on animal models, a therapeutic approach consisting of immune modulation through blockade of the NLRP3/IL-1 $\beta$  axis has been proposed for CMML with a *KRAS* mutation.<sup>9</sup> Clinical trials with novel NLRP3 blockers are starting to be developed to treat inflammatory diseases<sup>16</sup>; but so far, the only drugs approved for treating NLRP3-related diseases target IL-1 through either blocking antibodies (canakinumab) or recombinant IL-1 receptor antagonists (anakinra). Data regarding the efficacy of using these in-

hibitors in hematologic malignancies are limited to mouse models and *in vitro* studies.<sup>9,17,18</sup> This is not a minor issue, as allogeneic hematopoietic stem cell transplantation (HSCT), the only curative treatment available,<sup>19</sup> is rarely feasible for most CMML patients.<sup>20,21</sup> In addition, hypomethylating agents, the only approved therapy, have dismal response rates in the MP subtype.<sup>22</sup>

Our aim was to study the mechanisms underlying NLRP3/IL-1 $\beta$  axis disruption and *RAS* mutations in patients with CMML and to analyze the clinical efficacy of IL-1 $\beta$  inhibitors in this setting. We demonstrate in a cohort of CMML *KRAS*<sup>mut</sup> a basal oligomerization of the inflammasome, and that even when NLRP3 inhibition or IL-1R blockade could not eliminate the malignant clone, this therapy was able to reduce the inflammatory symptoms in a CMML *KRAS*<sup>G12D</sup> patient and facilitate clinical improvement, making potentially curative treatments, such as HSCT, possible.

## RESULTS

### The index patient

The index patient was a hypertensive male diagnosed in July 2020, at the age of 54 years, of a high-risk CMML-2, MP variant with a *KRAS*<sup>G12D</sup> mutation. At the age of 45 years, he had suffered from revascularized ischemic heart disease. His medical history was characterized by recurrent episodes of cellulitis (n = 3) and one episode (in 2019) of effusive-constrictive pericarditis accompanied by pleural effusion and right heart failure. He presented persistent monocytosis, anemia, thrombocytopenia, and splenomegaly. Cytogenetic, fluorescence *in situ* hybridization (–5/del5q and –7/del7q, PDGFR alpha/beta, and FGFR-1) and molecular (*JAK2*, *CALR*, *MPL*, *ASXL1*, *KIT*, and *BCR::ABL1*) studies found no relevant findings. Sequencing by gene panel related to myeloid disorders, however, revealed the presence of the c.35G>A, p.G12D variant in the *KRAS* gene (allelic burden of 48.9%). A PB smear and bone marrow (BM) aspirate/biopsy showed atypical monocytes, marked dysplastic features, and 11% of immature elements between myeloblasts, monoblasts, and promonocytes (Figure S1A), with CD123-positive cell clusters (Figure S1B), findings compatible with the diagnosis of *KRAS*<sup>G12D</sup> CMML-2 (based on the percentage of blasts and promonocytes in BM) (Table S1, patient #1). Although the morphological examination of the BM ruled out the presence of vacuoles in myeloid and erythroid precursor cells, as it has been recently described that some CMMLs co-occur with VEXAS syndrome,<sup>23</sup> exome sequencing data were used to discard the presence of mutations in *UBA1*.

At that time, the patient presented constitutional syndrome, and treatment with low-dose corticosteroids and subsequently with colchicine for constrictive pleuropericarditis was started. Unfortunately, colchicine treatment was discontinued early due to digestive intolerance. Between October and November 2020, the patient suffered new episodes of autoinflammation—orchiepididymitis, pneumonitis, and cellulitis (Figure 1A). A study of inflammatory parameters was performed afterward, showing that IL-1 $\beta$  release from PB mononuclear cells (PBMCs) was elevated compared to healthy donors (Figure 1B).

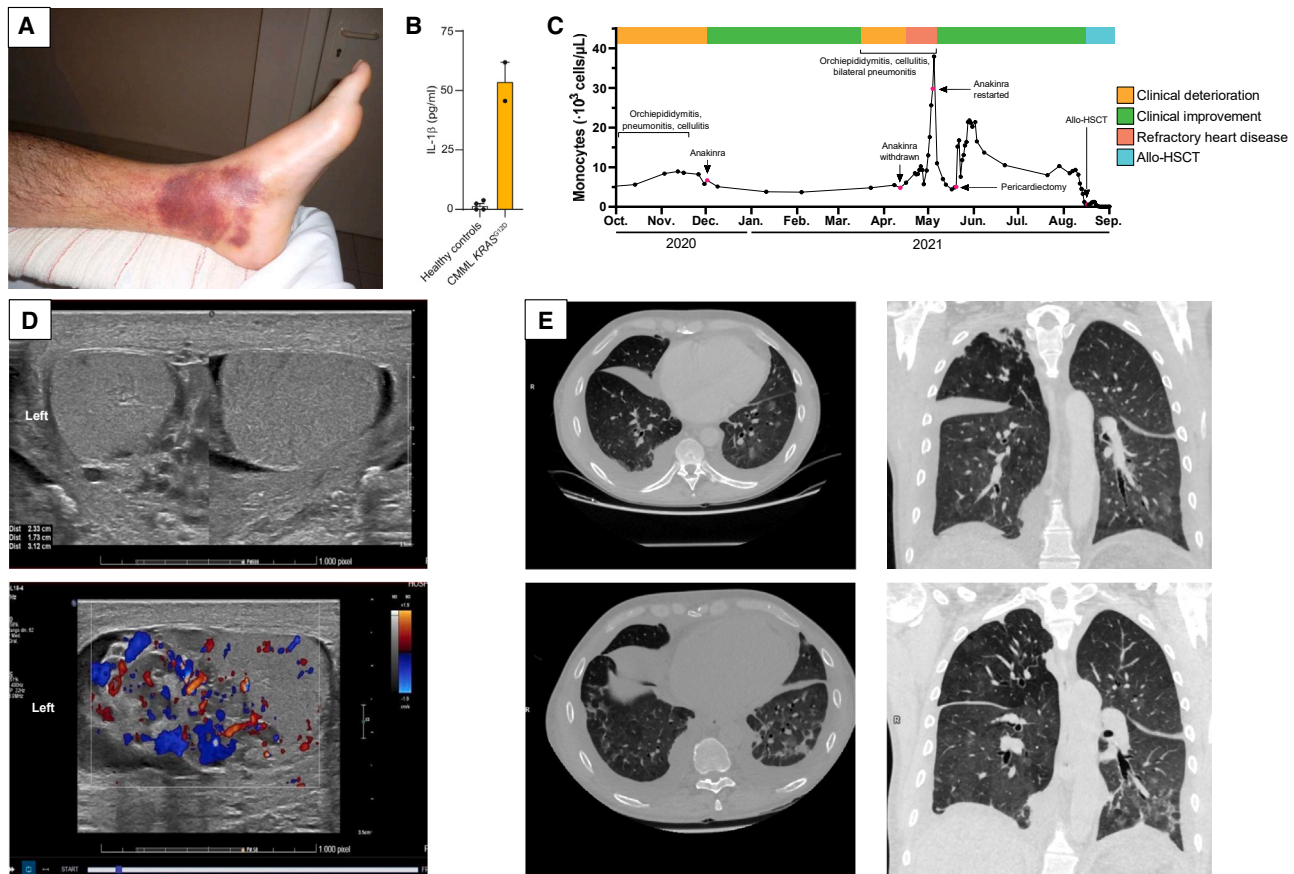


**Figure 1. Evolution of autoinflammatory episodes and levels of IL-1 $\beta$  of CMML  $KRAS^{G12D}$  patient treated with anakinra**

(A) Picture of the cellulitis episode on the lower legs of the index patient.

(B) Interleukin-1 $\beta$  release from peripheral blood (PB) mononuclear cells from healthy donors ( $n = 4$ , each dot represents an independent donor) and the index patient with a  $KRAS^{G12D}$  mutation before anakinra treatment (each dot represents a technical replicate). Data are represented as mean  $\pm$  SEM.

(C) Evolution of PB monocytes count during the evolution of the index patient. After introduction of anakinra, the patient was free of autoinflammatory episodes for 4 months, after which new episodes of autoinflammation occurred and anakinra was discontinued. Three weeks later, with constrictive pericarditis and congestive heart failure refractory to all therapeutic measures taken, associated with congestive nephropathy and cryptogenic organized pneumonia, in critical life-threatening condition, anakinra was reintroduced. Note the decrease of monocyte count in response to anakinra treatment (both the first time and when restored).

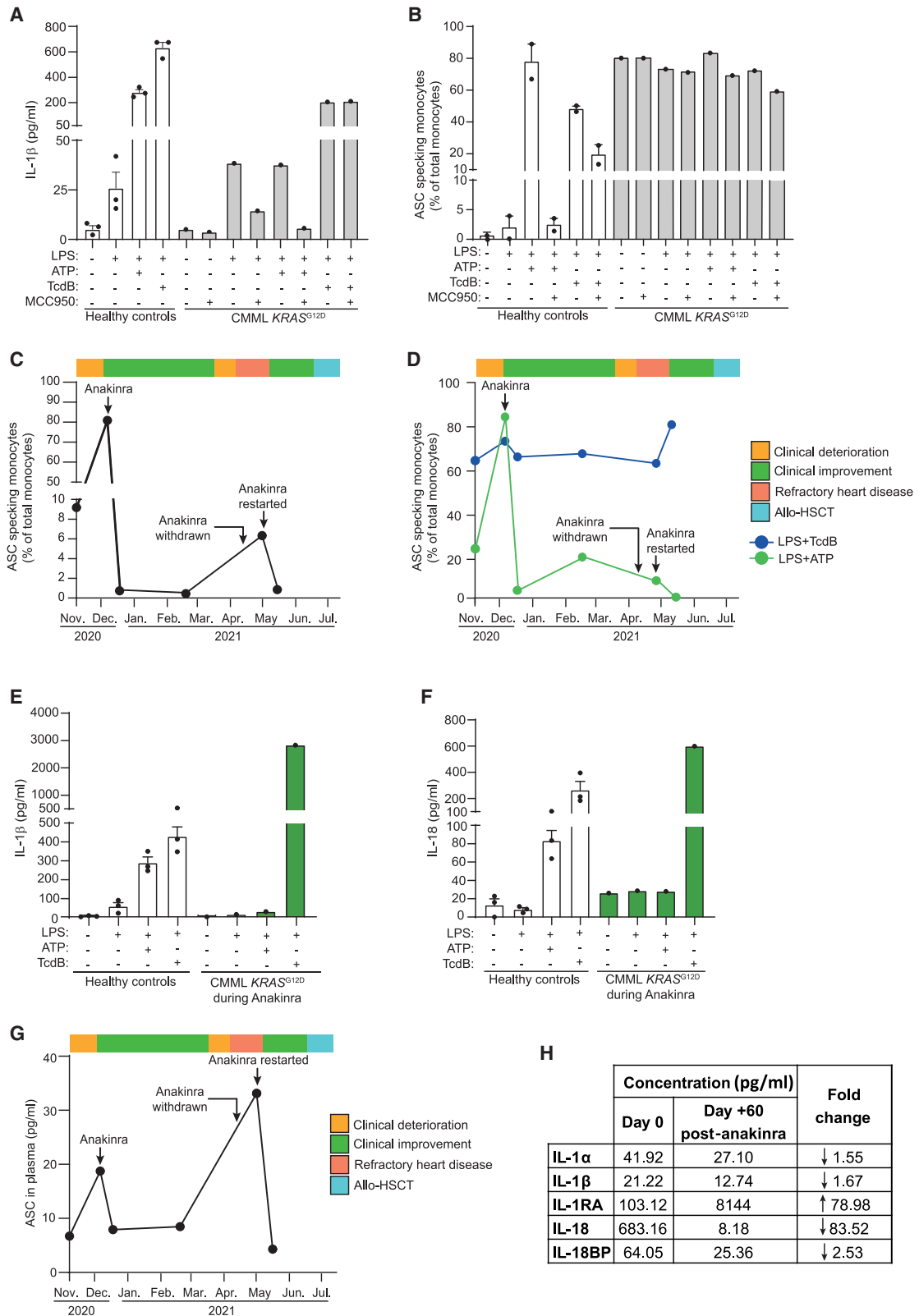
(D) Left orchiepididymitis. Left testicle  $27 \times 26 \times 32$  mm in size, with heterogeneous echogenicity. The color Doppler flow is increased. The epididymis is enlarged and vascularized. Diffuse edema of the subcutaneous cellular tissue in the left hemiscrotal. The right testicle is smaller ( $18 \times 26 \times 26$  mm) and shows a normal vascularization.

(E) Computed tomography of the chest with contrast: axial plane (left) and coronal plane (right). Top (08/04/2021): multiple bilateral pseudonodular ground-glass lung opacities associated with bilateral pleural effusion. Bottom (20 days later): bilateral parenchymal involvement with extensive ground glass areas. In the lower left lobe, there was an increase in the radiodensity of the pre-existing opacities with multiple peripheral consolidations that were not seen in the previous study. Moderate bilateral pleural effusion, which enters through the fissures, had worsened slightly compared to the previous study. Mild pericardial thickening of up to 3 mm.

### Blockade of IL-1R with anakinra as a bridge therapy to allogeneic HSCT

Given the impossibility of performing HSCT at that time (second wave of the coronavirus pandemic, COVID-19), 5 months after diagnosis, among the available anti-inflammatory drugs, anakinra (100 mg/day subcutaneous, s.c.) was chosen because of its direct inhibitory action on the IL-1 receptor. Treatment was started with good clinical response (weight gain), monocyte count stabilization (Figure 1C), and no toxicity. The patient remained clinically stable for 4 months, until he presented new episodes of autoinflammation with or-

chiepididymitis (Figure 1D), cellulitis, and bilateral pneumonitis (Figure 1E, top panel). Empirical antibiotic treatment was started, and anakinra was discontinued. Due to worsening pulmonary opacities (Figure 1E, bottom panel) and severe right heart failure, he required hospital admission. Despite intensive diuretic treatment and corticosteroid boluses due to the life-threatening situation (cardiopulmonary decompensation due to constrictive pericarditis, Figures S1C–S1F), anakinra was restarted 3 weeks after discontinuation. After stabilization, a successful pericardiectomy was performed, and the patient, in August 2021, was able to undergo HSCT of a



(legend on next page)

haploidentical sibling without major complications. Currently, the patient is alive and in remission, with no clinical signs of autoinflammation and with normal monocytes count in PB and complete chimera.

### Anakinra treatment attenuates NLRP3 inflammasome activity

Since PBMCs from the index patient constitutively released IL-1 $\beta$  before anakinra treatment (Figure 1B), we aimed to find out whether this release was dependent on inflammasome activation. We cultured PBMCs from the index patient obtained just before anakinra administration and unstimulated or stimulated with LPS (lipopolysaccharide), LPS+ATP (adenosine triphosphate) for the NLRP3 inflammasome, or LPS+TcdB (*Clostridium difficile* toxin B) for the pyrin inflammasome. In PBMCs from the index patient, the treatment with the NLRP3 inflammasome-specific blocker MCC950 decreased IL-1 $\beta$  release in all conditions, except under stimulation of pyrin inflammasome (LPS+TcdB) (Figure 2A). In contrast to healthy controls, in PBMCs from the index patient, we did not observe increased IL-1 $\beta$  release with the LPS+ATP combination versus with LPS alone but did upon activation of the pyrin inflammasome with LPS+TcdB (Figure 2A), suggesting maximal constitutive activation of NLRP3.

We next analyzed the presence of an ASC oligomer or speck in monocytes as a direct readout of active inflammasome formation by flow cytometry.<sup>24,25</sup> Surprisingly, our findings revealed that most monocytes from the pre-anakinra sample from the index patient presented ASC speck under resting conditions, and stimulation of the NLRP3 or pyrin inflammasomes was not able to further induce changes (Figure 2B). As expected, in healthy donors, ASC oligomerization occurred only after NLRP3 inflammasome activation with LPS+ATP or pyrin inflammasome activation with LPS+TcdB (Figure 2B). For representative assays, see Figures S2A–S2D. In the index patient samples, application of MCC950 after priming with LPS, and before ATP or TcdB, was not able to reduce the percentage of monocytes with speck of ASC (Figure 2B), consistent with the fact that ASC oligomerization is an irreversible final step in inflammasome activation and, in this case, had already been induced before activation of NLRP3 or pyrin by ATP or TcdB, respectively. This could also explain the small release of IL-1 $\beta$  after NLRP3 or pyrin activation compared with healthy donors (Figure 2A).

Importantly, after the first administration of anakinra, the percentage of basal ASC-specking monocytes of the index patient decreased and remained low at two time points examined during

that treatment (Figure 2C), while the patient was clinically stable (Figure 1C). Coinciding with new episodes of autoinflammation and discontinuation of anakinra, the percentage of ASC-specking monocytes increased, and it decreased again after reintroduction of anakinra (Figure 2C). Furthermore, this therapy also favored the reduction of monocytes with ASC speck when the NLRP3 inflammasome was activated, *ex vivo*, by LPS+ATP (Figure 2D). In contrast, the percentage of monocytes with ASC speck formation after activation of the pyrin inflammasome remained above 60% before and after anakinra treatment (Figure 2D). Accordingly, during such treatment, IL-1 $\beta$  and IL-18 release was not induced after *ex vivo* PBMC stimulation with LPS or LPS+ATP, but it was provoked when the pyrin inflammasome was activated by LPS+TcdB (Figures 2E and 2F). During anakinra treatment, PBMCs from the index patient also showed increased tumor necrosis factor alpha (TNF- $\alpha$ ) and IL-6 levels after stimulation with LPS, but this increase was less than that observed in PBMCs from healthy controls (Figure S2E). Altogether, these data suggest that blockade of the IL-1 pathway with anakinra can dampen the basal activation of the NLRP3 inflammasome but not the activation of the pyrin inflammasome.

Since it is known that inflammasome activation can lead to the release of ASC specks through pyroptosis,<sup>11,12</sup> we next measured ASC in the patient's plasma. We found that the ASC plasma levels decreased after anakinra and during periods of clinical improvement under this therapy (Figure 2G). The elevation of ASC in the plasma before anakinra treatment and after anakinra withdrawal (Figure 2G) correlates with the increase of monocytes with ASC speck in basal conditions (Figure 2C), suggesting that during periods of high ASC-specking monocytes, pyroptosis could be occurring *in vivo* in the patient and releasing ASC.

Accordingly, after treatment with anakinra, the levels of pro- and anti-inflammatory cytokines of the IL-1 family (IL-1 $\alpha$ , IL-1 $\beta$ , IL-18, and IL-18 binding protein [IL-18BP]) also decreased in the patient's plasma, whereas, in accordance with the mechanism of action of this agent, plasma levels of the IL-1 receptor antagonist (IL-1RA) increased (Figure 2H). Taken together, these data support that *in vivo* blockade of IL-1 signaling with anakinra in CMML *KRAS*<sup>mut</sup> patients can reduce NLRP3 inflammasome overactivation and its deleterious inflammatory outcomes.

### Clinical-biological characteristics of the cohort of CMML and MDS/MPN *KRAS*<sup>mut</sup> patients

Based on the findings found in the index patient, we wondered whether other patients with CMML or MDS/MPN and *KRAS*<sup>mut</sup>

#### Figure 2. Anakinra treatment reduces NLRP3 inflammasome activation

(A and B) Release of IL-1 $\beta$  from peripheral blood mononuclear cells (A) and percentage of ASC-specking monocytes (B), at baseline or after canonical activation of NLRP3 (LPS+ATP) and pyrin (LPS+TcdB) inflammasome, in the absence/presence of MCC950 from healthy donors ( $n = 2-3$ , each dot represents an individual donor, white bars) and the index patient with the *KRAS*<sup>G12D</sup> mutation before anakinra administration (gray bars).

(C) Percentage of monocytes with an ASC oligomer from the index patient over the time points examined before and after anakinra treatment.

(D) Percentage of monocytes with an ASC oligomer from the index patient after canonical NLRP3 inflammasome activation with LPS+ATP (green) or pyrin inflammasome activation with LPS+TcdB (dark blue) over the time points examined before and after anakinra treatment.

(E and F) Release of IL-1 $\beta$  (E) and IL-18 (F) from peripheral blood mononuclear cells, at baseline or treated, as indicated for NLRP3 (LPS+ATP) or pyrin (LPS+TcdB) inflammasome canonical activation, in healthy donors ( $n = 3$ , each dot represents an individual donor, white bars) and the index patient during anakinra treatment (green bars).

(G) Plasma levels of ASC in the index patient along the time points examined before and after anakinra treatment.

(H) Concentration of IL-1 family cytokines in the plasma of the CMML *KRAS*<sup>G12D</sup> index patient in response to anakinra.

For (A)–(F), are represented as mean  $\pm$  SEM, and each dot represents an individual donor.

would have similar biological characteristics. To address this hypothesis, we sought the collaboration of participants from the Spanish Group of Molecular Biology in Hematology (GBMH). We retrospectively identified 19 patients. Patients' clinical-biological characteristics are summarized in Tables S1 and S2. According to WHO criteria, *KRAS*<sup>mut</sup> patients were diagnosed with unclassifiable MDS/MPN (n = 1) and CMML (n = 18) 55.6% (10/18) MP subtype.<sup>1,2</sup>

Cytogenetic study (CG) was available in 18 of the 19 patients, three of them (16.7%) (#4, 17, 18) belonged to the intermediate/high CG risk group.<sup>7</sup> Regarding molecular studies, we found 20 *KRAS* mutations in the 19 patients, the majority (19/20) in exon 2, with p.G12D being the most frequent. One patient (#15) harbored two mutations: p.G60D (exon 3) and p.G12R (exon 2). Interestingly, five patients (26.3%) had mutations in other genes of the RAS pathway, specifically in *NRAS* (n = 7). Moreover, 12 of 19 patients (63.2%) had mutations in other myeloid genes, with *TET2*, *SRSF2*, and *ASXL1* being the most frequent.

Prior to the diagnosis, or during follow-up, 10 of the 19 patients had autoinflammation and/or autoimmunity (Table S1). The most frequent were adenitis (5/19), including a Rosai-Dorfman disease (#11), thyroid diseases (#11, 12, 19), and pneumonitis, pleuropericarditis, and cellulitis (#1, 2). Three patients suffered more than one episode of autoinflammation (#1, 2, 11), with a median time between the onset of autoinflammatory episodes and the diagnosis of CMML of 5 years. Positive autoantibodies were detected in two of the seven patients (#3, 4) for whom this information was available.

While seven of the patients remain under observation, 12 received some form of hematological treatment; and four underwent allogeneic HSCT (#1, 5, 8, 18). With a median follow-up of 20 months, 42.1% of patients (8/19) had died.

### NLRP3 inflammasome is activated in CMML *KRAS*<sup>mut</sup> patients

For the inflammasome studies, fresh samples from treatment-free patients were required. We were able to collect and analyze fresh PB samples from five patients in the CMML *KRAS*<sup>mut</sup> cohort (Table S1, #1, #3, #9, #11, #14) and from four CMML *KRAS*<sup>wt</sup> patients (Table S3, #20, #21, #28, #29).

Similar to the index case, all CMML *KRAS*<sup>mut</sup> patients had a significantly increased percentage of ASC-specking monocytes under resting and LPS priming conditions compared to healthy individuals and CMML *KRAS*<sup>wt</sup> patients (Figure 3A). In CMML *KRAS*<sup>mut</sup> patients, stimulation of the NLRP3 inflammasome was not able to increase the percentage of monocytes with ASC oligomers, suggesting that monocytes that could respond to NLRP3 activation were already activated, whereas pyrin inflammasome activation was able to increase the basal high percentage of ASC-specking monocytes, suggesting that there are some monocytes that were able to further activate pyrin but not NLRP3 inflammasome. In healthy donors and *KRAS*<sup>wt</sup> patients, by contrast, ASC oligomerization occurred only after activation of the NLRP3 or pyrin inflammasome with LPS+ATP or LPS+TcdB, respectively (Figure 3A). Basal and induced IL-1 $\beta$  release with LPS and LPS+ATP in *KRAS*<sup>mut</sup> patients was reduced by blocking the NLRP3 inflammasome with MCC950

(Figure 3B). Consistent with its specificity on the NLRP3 inflammasome, MCC950 was not able to significantly reduce IL-1 $\beta$  or ASC levels after activation of the pyrin inflammasome with LPS+TcdB (Figures 3B and 3C). Except for the pyrin inflammasome, the percentage of ASC-specking monocytes tended to decrease with MCC950, and this decrease was statistically significant when the NLRP3 inflammasome was activated (Figure 3C). However, after MCC950 treatment, over 30% of monocytes remained with ASC speck (Figure 3C), in agreement with recent data demonstrating that this agent is effective on the inactive NLRP3 structure and is probably not able to affect the irreversible NLRP3-ASC oligomer already formed.<sup>26</sup> As expected, in our cohort of CMML patients, an increase percentage of circulating monocytes was found (Figure S2F), being in agreement with the increased myeloid colony formation and the defective apoptosis of monocytes in these patients.<sup>27,28</sup> When analyzing the GEO database: GSE135902,<sup>29</sup> we found that in CMML patients with *RAS*<sup>mut</sup>, there were less expression of gasdermin D gene, despite elevation of *NLRP3* and *IL1B* gene expression (Figure S2G). Also, extracellular LDH levels normalized to the percentage of monocytes did not increase in unstimulated cultured PBMCs from CMML patients with *KRAS*<sup>mut</sup> (Figure 3D). This suggests that despite a basal activation of the inflammasome in CMML *KRAS*<sup>mut</sup> monocytes, there could be a defective pyroptosis and a potential hyperactive state of the monocytes, where active inflammasome would result in IL-1 $\beta$  release from living cells.<sup>30–32</sup> Regardless of the viability of *in vitro* cultured CMML *KRAS*<sup>mut</sup> monocytes, in CMML patient's plasma, an increase in high-mobility group box 1 (HMGB1) and especially in the soluble form of the P2X purinoceptor 7 receptor (P2X7) in patients with a *KRAS* mutation was observed (Figure 3E), suggesting that *in vivo* pyroptosis or another type of cell death could be occurring in patients with CMML *KRAS*<sup>mut</sup>.

Next, we evaluate the status of NLRP3 inflammasome pathway coding genes in the index CMML *KRAS*<sup>mut</sup> patient by whole-exome sequencing. The presence of pathogenic variants in any of the inflammasome-associated genes was discarded (Table S4).

### Circulating levels of inflammatory cytokines in CMML *KRAS*<sup>mut</sup> patients

Since an increase of different markers associated with pyroptosis was observed in the plasma of CMML *KRAS*<sup>mut</sup> patients, we next compared whether the circulating profile of inflammatory cytokines was also different compared to controls. Our data showed that, compared to healthy controls, the CMML *KRAS*<sup>wt</sup> patients only showed statistical differences in IL-6 (Figures 4A and 4B). In contrast, CMML *KRAS*<sup>mut</sup> patients displayed significantly higher levels of inflammasome- and nuclear factor kappa B (NF- $\kappa$ B)-associated cytokines (IL-1 $\alpha$ , IL-1RA, IL-12 p40, and IL-18) and lower levels of MCP-1 than healthy controls and CMML *KRAS*<sup>wt</sup> patients (Figures 4A and 4B). IL-18 was the cytokine with the largest differences: 28.4  $\pm$  7.9 vs. 1,287.0  $\pm$  762.8 pg/mL in CMML *KRAS*<sup>wt</sup> and *KRAS*<sup>mut</sup> patients, respectively (p < 0.01) (Table S5).

As we expected, our results demonstrate that CMML *KRAS*<sup>mut</sup> patients had significantly higher levels of IL-1 $\alpha$ , IL-1 $\beta$ , IL-12 p40, and IL-12 p70, but lower levels of IL-6 and MCP-1, than sepsis

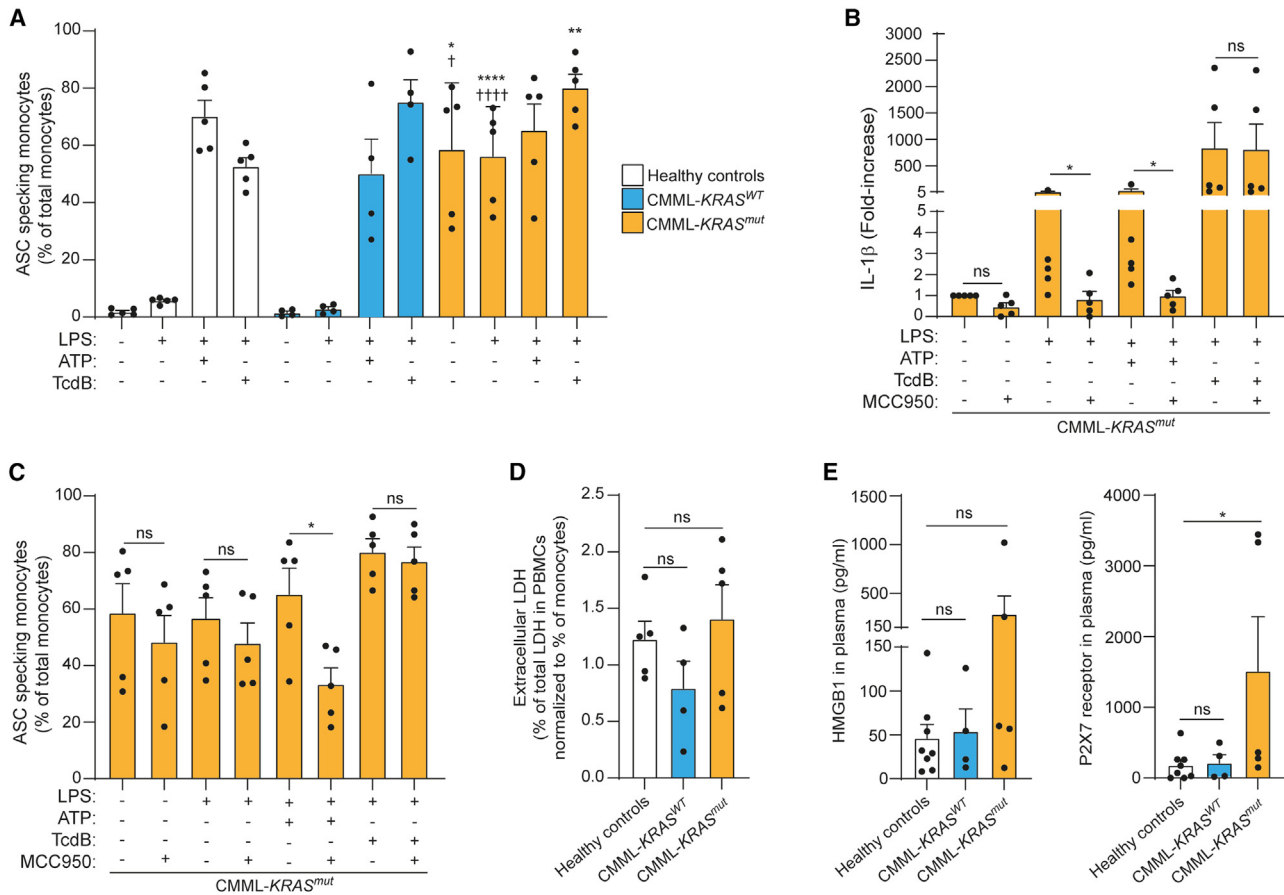


**Figure 3. Monocytes from CMML *KRAS*<sup>mut</sup> patients present a constitutive inflammasome activation**

(A) Percentage of ASC-specking monocytes in healthy controls (white bars), CMML patients without *KRAS* mutation (*KRAS*<sup>wt</sup>, blue bars), and CMML patients with a *KRAS* mutation (*KRAS*<sup>mut</sup>, orange bars) at baseline or treated as indicated for NLRP3 (LPS+ATP) or pyrin (LPS+TcdB) inflammasome activation.

(B and C) Release of IL-1β from peripheral blood mononuclear cells (PBMCs) (B) and the formation of ASC specks in monocytes (C) in CMML *KRAS*<sup>mut</sup> patients at baseline or after the indicated stimulation or treatment (LPS+ATP and LPS+TcdB for NLRP3 or pyrin inflammasome, respectively), in the absence/presence of MCC950. (B) Fold increase was calculated to control non-stimulated conditions, where the average of the higher value used to calculate fold increase is 1,066.58 pg/mL.

(D) Percentage of extracellular LDH from untreated PBMCs from healthy donors (white bar), *KRAS*<sup>wt</sup> patients (blue bar), and *KRAS*<sup>mut</sup> patients (orange bar). Data are normalized to the percentage of monocytes.

(E) Plasma concentration of HMGB1 and P2X7 receptor from healthy donors (white bar), *KRAS*<sup>wt</sup> patients (blue bar), and *KRAS*<sup>mut</sup> patients (orange bar).

For (A)–(E), data are represented as mean ± SEM; each dot represents an individual patient; ordinary one-way ANOVA test (two-tailed) was used for (A) (\* compares CMML *KRAS*<sup>mut</sup> vs. healthy controls; † compares CMML *KRAS*<sup>mut</sup> vs. CMML *KRAS*<sup>wt</sup>), and two-tailed t test in (B)–(E). Note that \* or †p < 0.05; \*\*p < 0.01; \*\*\*p < 0.001; \*\*\*\* or ††††p < 0.0001; ns, no significant difference (p > 0.05).

patients (as disease controls with acute inflammation) (Figure 4A; Table S5). Overall, in agreement with the activation of the NLRP3 inflammasome, CMML *KRAS*<sup>mut</sup> patients present an increase of circulating inflammasome-dependent cytokines.

Moreover, genetic and/or biological parameters other than *KRAS* mutation that could influence the higher cytokine levels observed in CMML *KRAS*<sup>mut</sup> patients were investigated. Thus, in the full CMML patient cohort (n = 17), we observed that none of the elevated cytokines in CMML *KRAS*<sup>mut</sup> (vs. *KRAS*<sup>wt</sup>) patients (IL-1α, IL-1RA, IL-12 p40 and p70, and IL-18) was significantly different when comparing patients according to the presence or absence of the most frequently found mutations (*TET2*, *SRSF2*, or *ASXL1*) or CMML variant (MP vs. MD) (Table S6).

## DISCUSSION

*RAS* mutations are found in 20%–30% of all human malignancies, such as CMML (7%–22%)<sup>33,34</sup> and juvenile myelomonocytic leukemia (20%–25%),<sup>1,2,34</sup> and mainly affect codons 12 and 13 of exon 2. Mutations in key residues in exon 2 or exon 3 (positions 10–14 [P loop region] and 58–72 [Switch-II region]) affect the GTP-binding site, preventing the conversion of the active RAS-GTP into inactive RAS-GDP,<sup>35,36</sup> leading to the continued activation of its downstream targets MEK1/2 and ERK1/2,<sup>37</sup> promoting cell proliferation and survival. However, since the RAS/RAF/MEK/ERK cascade couples cell surface receptor signals to transcription factors in both malignant and non-malignant immune cells,<sup>38</sup> recent studies have attempted



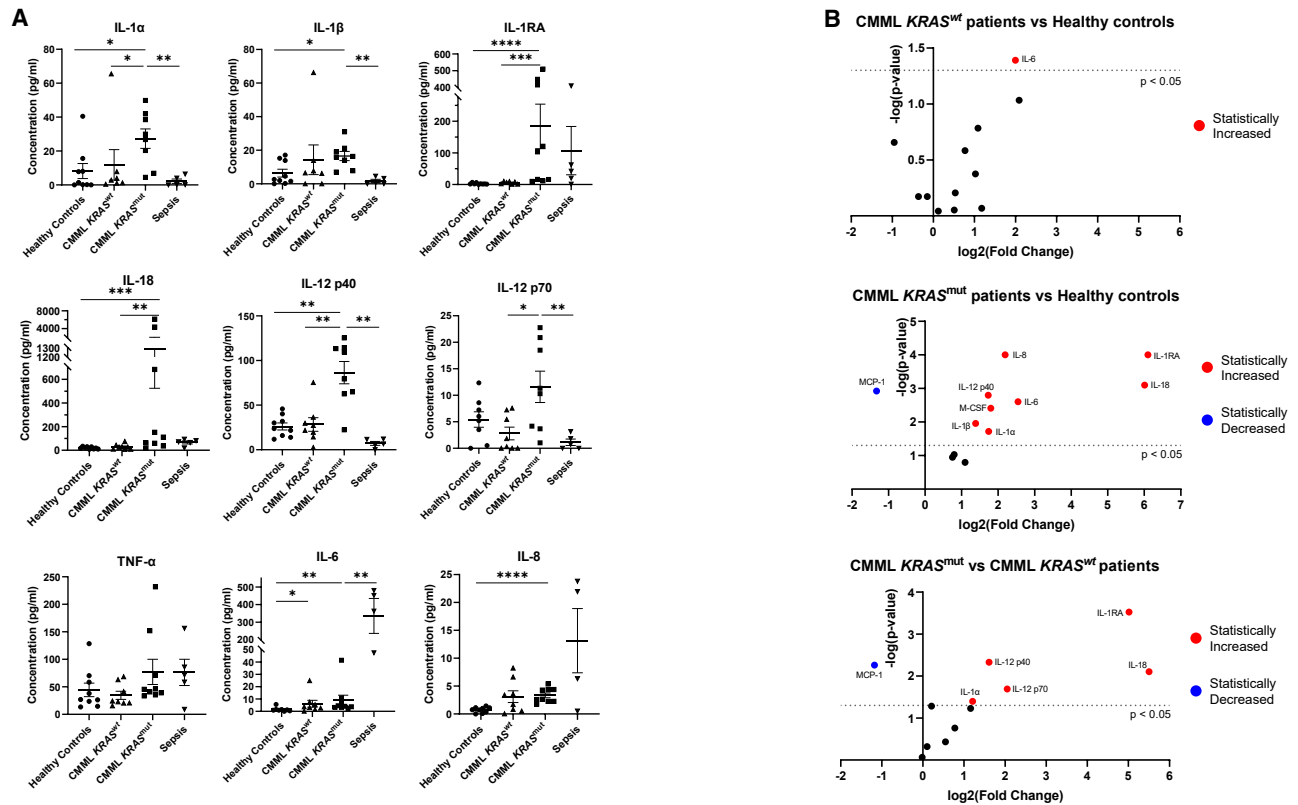


**Figure 4. Plasma cytokines in CMML patients**

(A) Plasma concentration of IL-1 $\alpha$ , IL-1 $\beta$ , IL-1RA, IL-18, IL-12 p40 and IL-12 p70, TNF- $\alpha$ , IL-6, and IL-8. Data are represented as mean  $\pm$  SEM. Each dot represents an individual patient. Mann-Whitney U test (two-tailed) was used to compare between groups: *KRAS*<sup>mut</sup> (n = 9) and *KRAS*<sup>wt</sup> patients (n = 8), healthy controls (n = 9), and patients with sepsis (n = 5, as control of acute inflammation). Outliers were detected in the datasets by the Grubbs' test ( $\alpha = 0.001$ ). \* $p < 0.05$ ; \*\* $p < 0.01$ ; \*\*\* $p < 0.001$ ; \*\*\*\* $p < 0.0001$ .

(B) Plasma cytokine concentration showing significant differences observed when comparing CMML *KRAS*<sup>wt</sup> vs. healthy controls, CMML *KRAS*<sup>mut</sup> vs. healthy controls, and CMML *KRAS*<sup>mut</sup> vs. CMML *KRAS*<sup>wt</sup> (Volcano plots). The x axis represents log<sub>2</sub> (fold change) and the y axis represents the negative log (p value). Statistically increased (red) was considered when  $p < 0.05$  and fold change  $> 1$ , and statistically decreased (blue) was considered when  $p < 0.05$  and fold change  $< 1$ . Each dot represents a cytokine, and the relevant ones are indicated. IL-2, IL-10, and GM-CSF were not detected in most patients.

to investigate whether myeloid clonal proliferation may be mediated not only by a direct oncogenic stimulus but also by inflammatory mechanisms.

The NLRP3 inflammasome has been implicated in different diseases, including MDS,<sup>16,18,39,40</sup> although this evidence comes mainly from models of NLRP3- or caspase-1-deficient mice or treating animals with experimental NLRP3 blockers.<sup>16,41</sup> Few studies address NLRP3 in the context of human disease, mainly due to the complexity of the signaling pathway, involving an NLRP3 oligomerization step to recruit ASC and activate caspase-1.<sup>42,43</sup> Basal ASC oligomerization has been found in MDS BM progenitor cells,<sup>39,40</sup> but it has not been found, so far, in unstimulated human circulating monocytes of any human disease. Here, we describe that in *KRAS*<sup>mut</sup> CMML, there is an increased percentage of circulating monocytes with ASC oligomers in PB under basal conditions. This result has not even been described for cryopyrin-associated periodic syndrome (CAPS) patients, who present gain-of-function mutations in NLRP3. Monocytes of CAPS patients increase the percentage of ASC-specking monocytes af-

ter LPS stimulation, avoiding the second signal of NLRP3 activation.<sup>44–46</sup> The NLRP3 inflammasome is a cellular irreversible mechanism once ASC oligomerizes, and since CMML monocytes already present ASC oligomers at the basal level, NLRP3 inhibition will not be able to block these already formed inflammasomes. The identification of the inflammasome sensor behind the ASC oligomer found in monocytes from CMML *KRAS*<sup>mut</sup> patients is a challenging question; upon culturing blood with the specific NLRP3 blocker MCC950,<sup>26,46–48</sup> the percentage of monocytes with ASC oligomers slightly decreases, while IL-1 $\beta$  release is significantly affected. This, together with the fact that no increased IL-1 $\beta$  release was achieved after the canonical NLRP3 activation with LPS+ATP, supports the idea that mutations in *KRAS* might be inducing NLRP3 activation, as recently reported in a mouse model and in human leukemia cells with a *KRAS*<sup>G12D</sup> mutation.<sup>9</sup>

The basal activation of the inflammasome in CMML *KRAS*<sup>mut</sup> patients was not associated to a pyroptosis of the monocytes, as they could be cultured and were not releasing LDH, suggesting that IL-1 $\beta$  could be released from living hyperactive cells, a state of

the cell found in macrophages and dendritic cells after certain inflammasome stimulation conditions.<sup>30–32</sup> Defective pyroptosis of monocytes from CMML *KRAS*<sup>mut</sup> patients would support the high viability of the cells while producing IL-1 $\beta$  and could represent another mechanism of cell survival together with the defective apoptosis found in CMML monocytes.<sup>28</sup> However, in the patients' plasma, we found an increase of cell death markers such as HMGB1, ASC, and the P2X7 receptor. While we have recently found the latter in the supernatants of human PBMCs after inflammasome activation,<sup>49</sup> HMGB1 and ASC alarmins have been reported to be released from dying cells, including but not exclusively from pyroptotic cells.<sup>11,12,50,51</sup> ASC has been found elevated in the serum of patients with autoinflammatory diseases, in HIV-infected persons, as well as in the bronchoalveolar lavage of individuals with chronic obstructive pulmonary disease.<sup>11,12,50</sup> In myeloid neoplasia, Basiorka et al. showed increased ASC oligomers in plasma of MDS patients, especially in low-risk disease,<sup>40</sup> compared to patients with other hematological cancers, and they suggested that ASC specks in plasma could be a biomarker for the differential diagnosis of MDS versus other hematological cancers, including CMML.<sup>40</sup> Our results, however, would not support their use as a surrogate marker for MDS-specific pyroptosis. Consistent with basal NLRP3 inflammasome activation, CMML *KRAS*<sup>mut</sup> patients showed higher levels of inflammasome-associated cytokines (IL-1 $\alpha$ , IL-1 $\beta$ , and IL-18), compared to CMML *KRAS*<sup>wt</sup> patients. Also, higher levels of NF- $\kappa$ B pathway-associated cytokines (IL-6, IL-8, and IL-12) and M-CSF were evidenced compared to healthy controls. Our results agree with data analyzing other *KRAS* mutated cancers, in which an increase in some of these cytokines has been described.<sup>52</sup> Specifically, in CMML, Niyongere et al. found that mutations in genes involved in signaling pathways (*JAK2*, *NRAS*, *KRAS*, *CBL*) had higher plasma levels of IL-12 p40 and IL-1RA.<sup>53</sup>

Our findings also provide insights into possible novel therapeutic strategies in CMML *KRAS*<sup>mut</sup> patients, who have a poorer response to conventional treatments.<sup>22</sup> Extracellular oligomers of ASC propagate inflammasome-dependent inflammation<sup>11,12</sup> and could be pharmacologically disaggregated by a, very recently developed, nanobody that has been used in animal models of inflammation.<sup>13</sup> Pharmacological inhibition of NLRP3 suppressed pyroptosis and restored effective hematopoiesis *in vitro* and *in vivo* in a mouse model of MDS.<sup>39</sup> Our study supports the notion that CMML *KRAS*<sup>mut</sup> patients could be candidates for therapies directed not only against NLRP3 but also against extracellular ASC oligomers. Although some NLRP3 blockers are entering early clinical trials, they are not yet approved for clinical use, and the only treatments available for patients with inflammasomopathies are IL-1<sup>54</sup> blockers: anakinra and canakinumab. Here we show that treatment of a CMML *KRAS*<sup>G12D</sup>-mutated patient with anakinra not only improved clinical status and monocytic proliferation, but it also blocked NLRP3 inflammasome activation in *ex vivo* experiments. This suggests the interesting hypothesis that proliferation of malignant monocyte clones might depend on IL-1 signaling and that its blockade influences NLRP3 activation, with this cytokine probably being a positive regulator for NLRP3 priming and activation. In fact, it has been recently shown that IL-1 contributes to malignant myeloproliferation.<sup>55</sup>

Since mutations in *KRAS/NRAS* are not unique to patients with CMML, our findings could be extended to other myeloid diseases such as juvenile CMML, MDS, and AML with mutations in the RAS pathway. Indeed, Basiorka et al. found that NLRP3 inflammasome activation was responsible for many of the hallmarks of MDS, such as macrocytosis and ineffective hematopoiesis.<sup>39</sup> On the other hand, these authors found that mutations in other myeloid genes, beyond *RAS*, can also induce NLRP3 inflammasome activation (*U2AF1*, *SF3B1*, *SRSF2*, *ASXL1*, and *TET2*).<sup>39</sup> In our cohort of CMML patients in whom inflammasome studies were performed, four of the five *KRAS*<sup>mut</sup> patients had only *KRAS* mutation. In contrast, each of the four CMML *KRAS*<sup>wt</sup> patients carried a different mutational profile; and all of them presented mutations in splicing genes and epigenetic modifiers (*TET2*, *ASXL1*, and/or *SRSF2*), which occur in up to 80% of patients with CMML,<sup>1</sup> being, therefore, a representative sample of CMML patients. Given that genetically the main difference between the two cohorts of patients is the presence of mutations in *KRAS*, the high basal inflammasome activation that we observed in CMML *KRAS*<sup>mut</sup> patients can only be explained by aberrant *KRAS* signaling. However, due to the size of our cohort, we cannot rule out that mutations in myeloid genes other than *KRAS* may also influence inflammasome activation. In fact, previous studies have shown that the proportion of pyroptotic erythroid progenitors in BM samples from MDS patients increases with the complexity of the mutations and the allelic burden.<sup>39</sup> In line with these authors, the mean *KRAS*<sup>mut</sup> allele burden of the patients in our series in whom NLRP3 inflammasome study could be performed was higher than 40%. Among them, those with an allelic burden close to 50% were associated with repetitive and severe episodes of autoinflammation. This is not surprising, since the RAS/RAF/MEK/ERK pathway is also involved in the control of B cell tolerance and autoantibody production.<sup>56,57</sup> Consistent with our findings, very recently, Andina et al. have shown that NLRP3 dysregulation in CMML positively correlated with disease severity.<sup>58</sup>

Taken together, our study demonstrates using functional assays that in a cohort of CMML *KRAS*<sup>mut</sup> patients, there is a basal activation of the NLRP3 inflammasome and a specific inflammatory cytokine signature. At present, the IL-1R blocker (anakinra) may be a therapeutic option to be considered to improve the clinical status and to control monocytic proliferation and NLRP3 inflammasome activation. In the future, inflammasome blockade with different therapies may offer new opportunities for patients with myeloid neoplasms and *RAS* mutations.

### Limitations of the study

The principal limitation of the study is the small sample size of the cohort of primary CMML samples. According to that, (1) only a case report of a patient with *KRAS*<sup>mut</sup> CMML successfully quelled by anakinra treatment with subsequent bridging to allograft is presented; and (2) although our data suggest that only *KRAS*<sup>mut</sup> monocytes have constitutively activated the NLRP3 inflammasome, the cohort of *KRAS*<sup>wt</sup> patients is too small, and we cannot rule out that mutations in myeloid genes other than *KRAS* may have a similar effect on the NLRP3 inflammasome. Therefore, it would be interesting to (1) study additional samples in the experimental studies (both from *KRAS*<sup>mut</sup> and *KRAS*<sup>wt</sup> CMML

patients); (2) to expand the subgroup comparisons to MAPK-mutated cases, cases with mutations in other RAS pathway genes (*NRAS*, *CBL*, and *PTPN11*), or signaling-related genes beyond RAS pathway; and (3) finally, to observe the impact of the newly available specific inhibitors of KRAS on *in vitro* experiments to activate the NLRP3 inflammasome.

## STAR★METHODS

Detailed methods are provided in the online version of this paper and include the following:

- **KEY RESOURCES TABLE**
- **RESOURCE AVAILABILITY**
  - Lead contact
  - Materials availability
  - Data and code availability
- **EXPERIMENTAL MODEL AND STUDY PARTICIPANT DETAILS**
  - Patients and cohorts
  - Human clinical samples
- **METHOD DETAILS**
  - Cells and treatments
  - Evaluation of monocytes with ASC by flow cytometry
  - Lactate dehydrogenase assay
  - Cytokine evaluation
  - Sequencing analysis
  - Whole exome sequencing
- **QUANTIFICATION AND STATISTICAL ANALYSIS**

## SUPPLEMENTAL INFORMATION

Supplemental information can be found online at <https://doi.org/10.1016/j.xcrm.2023.101329>.

## ACKNOWLEDGMENTS

We are particularly grateful for the generous contribution of the patients and healthy donors. We would like to thank Lourdes Martínez and Juana M. Plascencia (Radiology Department) and Ma José López Poveda (Pathology Department) of the Hospital Morales-Meseguer for their help in the selection of the images, M.C. Baños and A.I. Gomez (IMIB) for technical support, and all the members of Dr. Pelegrín's laboratory for comments and suggestions. We are indebted to GBMH, Marta Martín (IBSAL, Salamanca), Mar Tormo (Clinic University Hospital, Valencia), and Ana Garrido (Sant Pau Hospital, Barcelona) for contributing to the execution of the present study. We also thank the collaboration of Biobank Network of the Region of Murcia, BIOBANC-MUR, registered on the Registro Nacional de Biobancos with registration number B.0000859. BIOBANC-MUR is supported by the Instituto de Salud Carlos III (grant PT20/00109), by Instituto Murciano de Investigación Biosanitaria, and by Consejería de Salud de la Comunidad Autónoma de la Región de Murcia.

This work was supported by grants to P.P. from MCIN/AEI/10.13039/501100011033 (grant PID2020-116709RB-I00), Fundación Séneca (grants 20859/PI/18, 21897/PI/22, and 21081/PDC/19), the Instituto de Salud Carlos III (grants DTS21/00080 and AC22/00009), the EU Horizon 2020 project PlasticHeal (grant 965196), and grants from the Instituto de Salud Carlos III and Fondo Europeo de Desarrollo Regional (FEDER) to F.F.-M. (PI21/00347). L.H.-N. was supported by Fellowship 21214/FPI/19 (Fundación Séneca, Región de Murcia, Spain). E.J.C.-Z. is supported by the Training of University Teachers Program (FPU18/03189). M.L.M. is supported by Next Generation EU grant (PMP21/00052). This study was approved by the Clinical Research Ethics Committee of the Hospital Universitario Morales-Meseguer (reference

no. 07/19). All patients and donors provided written informed consent in accordance with the Declaration of Helsinki.

## AUTHOR CONTRIBUTIONS

L.H.-N., H.M.-B., E.J.C.-Z., M.L.M., and R.T.-M.: experimental execution; L.M.-A., C.G.-P., and E.S.-E.: sample collection; L.H.-N., E.J.C.-Z., E.S.-E., R.T.-M., T.H.C.-L., F.F.-M., and P.P.: data analysis; L.H.-N. and E.J.C.-Z.: figure preparation. All other authors contributed to patient data and/or material for analysis. F.F.-M. and P.P. conceived the experiments, wrote the paper, and provided funding and overall supervision of the study. All authors approved the final version of the manuscript.

## DECLARATION OF INTERESTS

P.P. is consultant of Viva In Vitro Diagnostics SL. P.P., H.M.-B., and C.G.-P. are inventors on patent PCT/EP2020/056729. L.H.-N., L.M.-A., H.M.-B., C.G.-P., and P.P. are co-founders of Viva In Vitro Diagnostics SL but declare that the research was conducted in the absence of any commercial or financial relationships that could be construed as a potential conflict of interest.

Received: June 22, 2023

Revised: September 21, 2023

Accepted: November 17, 2023

Published: December 19, 2023

## REFERENCES

1. Arber, D.A., Orazi, A., Hasserjian, R., Borowitz, M.J., Calvo, K.R., Kvasnicka, H.M., Wang, S.A., Bagg, A., Barbui, T., Branford, S., et al. (2022). International Consensus Classification of Myeloid Neoplasms and Acute Leukemias: integrating morphologic, clinical, and genomic data. *Blood* **140**, 1200–1228.
2. Khoury, J.D., Solary, E., Abla, O., Akkari, Y., Alaggio, R., Apperley, J.F., Bejar, R., Berti, E., Busque, L., Chan, J.K.C., et al. (2022). The 5th edition of the World Health Organization Classification of Haematolymphoid Tumours: Myeloid and Histiocytic/Dendritic Neoplasms. *Leukemia* **36**, 1703–1719.
3. Reiter, A., Invernizzi, R., Cross, N.C.P., and Cazzola, M. (2009). Molecular basis of myelodysplastic/myeloproliferative neoplasms. *Haematologica* **94**, 1634–1638.
4. Kohlmann, A., Grossmann, V., Klein, H.U., Schindela, S., Weiss, T., Kazak, B., Dicker, F., Schnittger, S., Dugas, M., Kern, W., et al. (2010). Next-Generation Sequencing Technology Reveals a Characteristic Pattern of Molecular Mutations in 72.8% of Chronic Myelomonocytic Leukemia by Detecting Frequent Alterations in *TET2*, *CBL*, *RAS*, and *RUNX1*. *J. Clin. Oncol.* **28**, 3858–3865.
5. Carr, R.M., Vorobyev, D., Lasho, T., Marks, D.L., Tolosa, E.J., Vedder, A., Almada, L.L., Yurcheko, A., Padioleau, I., Alver, B., et al. (2021). RAS mutations drive proliferative chronic myelomonocytic leukemia via a KMT2A-PLK1 axis. *Nat. Commun.* **12**, 2901.
6. Itzykson, R., Kosmider, O., Renneville, A., Gelsi-Boyer, V., Meggendorfer, M., Morabito, M., Berthon, C., Adès, L., Fenaux, P., Beyne-Rauzy, O., et al. (2013). Prognostic Score Including Gene Mutations in Chronic Myelomonocytic Leukemia. *J. Clin. Oncol.* **31**, 2428–2436.
7. Such, E., Germing, U., Malcovati, L., Cervera, J., Kuendgen, A., Porta, D., Nomdedeu, B., Arenillas, L., Luño, E., Xicoy, B., et al. (2013). Development and validation of a prognostic scoring system for patients with chronic myelomonocytic leukemia. *Blood* **121**, 3005–3015.
8. McCubrey, J.A., Steelman, L.S., Chappell, W.H., Abrams, S.L., Wong, E.W.T., Chang, F., Lehmann, B., Terrian, D.M., Milella, M., Tafuri, A., et al. (2007). Roles of the Raf/MEK/ERK pathway in cell growth, malignant transformation and drug resistance. *Biochim. Biophys. Acta* **1773**, 1263–1284.

9. Hamarshesh, S., Osswald, L., Saller, B.S., Unger, S., De Feo, D., Vinnakota, J.M., Konantz, M., Uhl, F.M., Becker, H., Lübbert, M., et al. (2020). Oncogenic KrasG12D causes myeloproliferation via NLRP3 inflammasome activation. *Nat. Commun.* *11*, 1659.
10. Broz, P., Pelegrín, P., and Shao, F. (2020). The gasdermins, a protein family executing cell death and inflammation. *Nat. Rev. Immunol.* *20*, 143–157.
11. Baroja-Mazo, A., Martín-Sánchez, F., Gómez, A.I., Martínez, C.M., Amores-Iniesta, J., Compan, V., Barberà-Cremades, M., Yagüe, J., Ruiz-Ortiz, E., Antón, J., et al. (2014). The NLRP3 inflammasome is released as a particulate danger signal that amplifies the inflammatory response. *Nat. Immunol.* *15*, 738–748.
12. Franklin, B.S., Bossaller, L., De Nardo, D., Ratter, J.M., Stutz, A., Engels, G., Brenker, C., Nordhoff, M., Mirandola, S.R., Al-Amoudi, A., et al. (2014). The adaptor ASC has extracellular and “prionoid” activities that propagate inflammation. *Nat. Immunol.* *15*, 727–737.
13. Bertheloot, D., Wanderley, C.W., Schneider, A.H., Schifflers, L.D., Wuertth, J.D., Tödtmann, J.M., Maasewerd, S., Hawwari, I., Duthie, F., Rohland, C., et al. (2022). Nanobodies dismantle post-pyroptotic ASC specks and counteract inflammation *in vivo*. *EMBO Mol. Med.* *14*, e15415.
14. Groß, C.J., Mishra, R., Schneider, K.S., Médard, G., Wettmarshausen, J., Dittlein, D.C., Shi, H., Gorka, O., Koenig, P.A., Fromm, S., et al. (2016). K + Efflux-Independent NLRP3 Inflammasome Activation by Small Molecules Targeting Mitochondria. *Immunity* *45*, 761–773.
15. Tapia-Abellán, A., Angosto-Bazarrá, D., Alarcón-Vila, C., Baños, M.C., Hafner-Bratkovič, I., Oliva, B., and Pelegrín, P. (2021). Sensing low intracellular potassium by NLRP3 results in a stable open structure that promotes inflammasome activation. *Sci. Adv.* *7*, 4468–4483.
16. Coll, R.C., Schroder, K., and Pelegrín, P. (2022). NLRP3 and pyroptosis blockers for treating inflammatory diseases. *Trends Pharmacol. Sci.* *43*, 653–668.
17. Comont, T., Treiner, E., and Vergez, F. (2021). From Immune Dysregulations to Therapeutic Perspectives in Myelodysplastic Syndromes: A Review. *Diagnostics* *11*, 1982.
18. Sallman, D.A., and List, A. (2019). The central role of inflammatory signaling in the pathogenesis of myelodysplastic syndromes. *Blood* *133*, 1039–1048.
19. Robin, M., de Wreede, L.C., Padron, E., Bakunina, K., Fenaux, P., Koster, L., Nazha, A., Beelen, D.W., Rampal, R.K., Sockel, K., et al. (2022). Role of allogeneic transplantation in chronic myelomonocytic leukemia: an international collaborative analysis. *Blood* *140*, 1408–1418.
20. de Witte, T., Bowen, D., Robin, M., Malcovati, L., Niederwieser, D., Yakoub-Agha, I., Mufti, G.J., Fenaux, P., Sanz, G., Martino, R., et al. (2017). Allogeneic hematopoietic stem cell transplantation for MDS and CMML: recommendations from an international expert panel. *Blood* *129*, 1753–1762.
21. Patnaik, M.M., and Tefferi, A. (2018). Chronic myelomonocytic leukemia: 2018 update on diagnosis, risk stratification and management. *Am. J. Hematol.* *93*, 824–840.
22. Lasho, T., and Patnaik, M.M. (2021). Novel therapeutic targets for chronic myelomonocytic leukemia. *Best Pract. Res. Clin. Haematol.* *34*, 101244.
23. Zhao, L.P., Schell, B., Kim, R., Sébert, M., Lemaire, P., Boy, M., Mathis, S., Larcher, L., Chauvel, C., Dhouaieb, M.B., et al. (2021). MDS-029: Prevalence of VEXAS Syndrome in MDS/CMML Patients with Systemic Inflammation and Auto-Immune Disease. *Clin. Lymphoma, Myeloma & Leukemia* *21*, S337–S338.
24. Sester, D.P., Thygesen, S.J., Sagulenko, V., Vajjhala, P.R., Cridland, J.A., Vitak, N., Chen, K.W., Osborne, G.W., Schroder, K., and Stacey, K.J. (2015). A Novel Flow Cytometric Method To Assess Inflammasome Formation. *J. Immunol.* *194*, 455–462.
25. Hurtado-Navarro, L., Baroja-Mazo, A., Martínez-Banaclocha, H., and Pelegrín, P. (2022). Assessment of ASC Oligomerization by Flow Cytometry. In *The Inflammasome. Methods in Molecular Biology* 1-9, A.A. Abdul-Satter, ed.
26. Hochheiser, I.V., Pils, M., Hagelueken, G., Moecking, J., Marleaux, M., Brinkschulte, R., Latz, E., Engel, C., and Geyer, M. (2022). Structure of the NLRP3 decamer bound to the cytokine release inhibitor CRID3. *Nature (London, U. K.)* *604*, 184–189.
27. Geissler, K., Jäger, E., Barna, A., Alendar, T., Ljubuncic, E., Sliwa, T., and Valent, P. (2016). Chronic myelomonocytic leukemia patients with RAS pathway mutations show high *in vitro* myeloid colony formation in the absence of exogenous growth factors. *Leukemia* *30*, 2280–2281.
28. Sevin, M., Debeurme, F., Laplane, L., Badel, S., Morabito, M., Newman, H.L., Torres-Martin, M., Yang, Q., Badaoui, B., Wagner-Ballon, O., et al. (2021). Cytokine-like protein 1-induced survival of monocytes suggests a combined strategy targeting MCL1 and MAPK in CMML. *Blood* *137*, 3390–3402.
29. Franzini, A., Pomicter, A.D., Yan, D., Khorashad, J.S., Tantravahi, S.K., Than, H., Ahmann, J.M., O'Hare, T., and Deininger, M.W. (2019). The transcriptome of CMML monocytes is highly inflammatory and reflects leukemia-specific and age-related alterations. *Blood Adv.* *3*, 2949–2961.
30. Evavold, C.L., Ruan, J., Tan, Y., Xia, S., Wu, H., and Kagan, J.C. (2018). The Pore-Forming Protein Gasdermin D Regulates Interleukin-1 Secretion from Living Macrophages. *Immunity* *48*, 35–44.e6.
31. Zanoni, I., Tan, Y., Di Gioia, M., Broggi, A., Ruan, J., Shi, J., Donado, C.A., Shao, F., Wu, H., Springstead, J.R., and Kagan, J.C. (2016). An endogenous caspase-11 ligand elicits interleukin-1 release from living dendritic cells. *Science* *352*, 1232–1236.
32. Lieberman, J., Wu, H., and Kagan, J.C. (2019). Gasdermin D activity in inflammation and host defense. *Sci. Immunol.* *4*, eaav1447.
33. Itzykson, R., Fenaux, P., Bowen, D., Cross, N.C.P., Cortes, J., De Witte, T., Germing, U., Onida, F., Padron, E., Platzbecker, U., et al. (2018). Diagnosis and Treatment of Chronic Myelomonocytic Leukemias in Adults. *Hemisphere* *2*, e150.
34. Patnaik, M.M., and Lasho, T. (2020). Evidence-Based Minireview: Myelodysplastic syndrome/myeloproliferative neoplasm overlap syndromes: a focused review. *Hematology* *2020*, 460–464.
35. Johnson, C.W., Reid, D., Parker, J.A., Salter, S., Knihtila, R., Kuzmic, P., and Mattos, C. (2017). The small GTPases K-Ras, N-Ras, and H-Ras have distinct biochemical properties determined by allosteric effects. *J. Biol. Chem.* *292*, 12981–12993.
36. Pantsar, T. (2020). The current understanding of KRAS protein structure and dynamics. *Comput. Struct. Biotechnol. J.* *18*, 189–198.
37. Meynier, S., and Rieux-Laucat, F. (2020). After 95 years, it's time to eRASe JMML. *Blood Rev.* *43*, 100652.
38. Cobb, M.H., and Goldsmith, E.J. (1995). How MAP Kinases Are Regulated. *J. Biol. Chem.* *270*, 14843–14846.
39. Basiorka, A.A., McGraw, K.L., Eksioglu, E.A., Chen, X., Johnson, J., Zhang, L., Zhang, Q., Irvine, B.A., Cluzeau, T., Sallman, D.A., et al. (2016). The NLRP3 inflammasome functions as a driver of the myelodysplastic syndrome phenotype. *Blood* *128*, 2960–2975.
40. Basiorka, A.A., McGraw, K.L., Abbas-Aghababazadeh, F., McLemore, A.F., Vincelette, N.D., Ward, G.A., Eksioglu, E.A., Sallman, D.A., Ali, N.A., Padron, E., et al. (2018). Assessment of ASC specks as a putative biomarker of pyroptosis in myelodysplastic syndromes: an observational cohort study. *Lancet. Haematol.* *5*, e393–e402.
41. Mangan, M.S.J., Olhava, E.J., Roush, W.R., Seidel, H.M., Glick, G.D., and Latz, E. (2018). Targeting the NLRP3 inflammasome in inflammatory diseases. *Nat. Rev. Drug Discov.* *17*, 588–606.
42. Schmidt, F.I., Lu, A., Chen, J.W., Ruan, J., Tang, C., Wu, H., and Ploegh, H.L. (2016). A single domain antibody fragment that recognizes the adaptor ASC defines the role of ASC domains in inflammasome assembly. *J. Exp. Med.* *213*, 771–790.
43. Lu, A., Li, Y., Schmidt, F.I., Yin, Q., Chen, S., Fu, T.M., Tong, A.B., Ploegh, H.L., Mao, Y., and Wu, H. (2016). Molecular basis of caspase-1 polymerization and its inhibition by a new capping mechanism. *Nat. Struct. Mol. Biol.* *23*, 416–425.

44. Mensa-Vilaro, A., Bosque, M.T., Magri, G., Honda, Y., Martínez-Banaclocha, H., Casorran-Berges, M., Sintes, J., González-Roca, E., Ruiz-Ortiz, E., Heike, T., et al. (2016). Brief Report: Late-Onset Cryopyrin-Associated Periodic Syndrome Due to Myeloid-Restricted Somatic NLRP3 Mosaicism. *Arthritis Rheumatol* 68, 3035–3041.
45. Weber, A.N.R., Tapia-Abellán, A., Liu, X., Dickhöfer, S., Aróstegui, J.I., Pelegrín, P., Welzel, T., and Kuemmerle-Deschner, J.B. (2022). Effective *ex vivo* inhibition of cryopyrin-associated periodic syndrome (CAPS)-associated mutant NLRP3 inflammasome by MCC950/CRID3. *Rheumatology* 61, e299–e313.
46. Tapia-Abellán, A., Angosto-Bazarra, D., Martínez-Banaclocha, H., de Torre-Minguela, C., Cerón-Carrasco, J.P., Pérez-Sánchez, H., Arostegui, J.I., and Pelegrín, P. (2019). MCC950 closes the active conformation of NLRP3 to an inactive state. *Nat. Chem. Biol.* 15, 560–564.
47. Coll, R.C., Robertson, A.A.B., Chae, J.J., Higgins, S.C., Muñoz-Planillo, R., Inserra, M.C., Vetter, I., Dungan, L.S., Monks, B.G., Stutz, A., et al. (2015). A small-molecule inhibitor of the NLRP3 inflammasome for the treatment of inflammatory diseases. *Nat. Med.* 21, 248–255.
48. Coll, R.C., Hill, J.R., Day, C.J., Zamoshnikova, A., Boucher, D., Massey, N.L., Chitty, J.L., Fraser, J.A., Jennings, M.P., Robertson, A.A.B., and Schroder, K. (2019). MCC950 directly targets the NLRP3 ATP-hydrolysis motif for inflammasome inhibition. *Nat. Chem. Biol.* 15, 556–559.
49. García-Villalba, J., Hurtado-Navarro, L., Peñín-Franch, A., Molina-López, C., Martínez-Alarcón, L., Angosto-Bazarra, D., Baroja-Mazo, A., and Pelegrín, P. (2022). Soluble P2X7 Receptor Is Elevated in the Plasma of COVID-19 Patients and Correlates With Disease Severity. *Front. Immunol.* 13, 2207.
50. Ahmad, F., Mishra, N., Ahrenstorf, G., Franklin, B.S., Latz, E., Schmidt, R.E., and Bossaller, L. (2018). Evidence of inflammasome activation and formation of monocyte-derived ASC specks in HIV-1 positive patients. *AIDS (Phila.)* 32, 299–307.
51. de Torre-Minguela, C., Barberà-Cremades, M., Gómez, A.I., Martín-Sánchez, F., and Pelegrín, P. (2016). Macrophage activation and polarization modify P2X7 receptor secretome influencing the inflammatory process. *Sci. Rep.* 6, 22586.
52. Hamarsheh, S., Groß, O., Brummer, T., and Zeiser, R. (2020). Immune modulatory effects of oncogenic KRAS in cancer. *Nat. Commun.* 11, 5439.
53. Niyongere, S., Lucas, N., Zhou, J.M., Sansil, S., Pomictier, A.D., Balasis, M.E., Robinson, J., Kroeger, J., Zhang, Q., Zhao, Y.L., et al. (2019). Heterogeneous expression of cytokines accounts for clinical diversity and refines prognostication in CMML. *Leukemia* 33, 205–216.
54. Dinarello, C.A., Simon, A., and van der Meer, J.W.M. (2012). Treating inflammation by blocking interleukin-1 in a broad spectrum of diseases. *Nat. Rev. Drug Discov.* 11, 633–652.
55. Villatoro, A., Cuminetti, V., Bernal, A., Torroja, C., Cossio, I., Benguría, A., Ferré, M., Konieczny, J., Vázquez, E., Rubio, A., et al. (2023). Endogenous IL-1 receptor antagonist restricts healthy and malignant myeloproliferation. *Nat. Commun.* 14, 12.
56. Teodorovic, L.S., Babolin, C., Rowland, S.L., Greaves, S.A., Baldwin, D.P., Torres, R.M., and Pelanda, R. (2014). Activation of Ras overcomes B-cell tolerance to promote differentiation of autoreactive B cells and production of autoantibodies. *Proc. Natl. Acad. Sci. USA* 111, E2797–E2806.
57. Meynier, S., and Rieux-Laucat, F. (2019). FAS and RAS related Apoptosis defects: From autoimmunity to leukemia. *Immunol. Rev.* 287, 50–61.
58. Andina, N., de Meuron, L., Schnegg-Kaufmann, A.S., Sarangdhar, M.A., Ansermet, C., Bombaci, G., Batta, K., Keller, N., Porret, N.A., Angelillo-Scherrer, A., et al. (2023). Increased Inflammasome Activation Is Associated with Aging and Chronic Myelomonocytic Leukemia Disease Severity. *J. Immunol.* 210, 580–589.

STAR★METHODS

KEY RESOURCES TABLE

REAGENT or RESOURCE	SOURCE	IDENTIFIER
<b>Antibodies</b>		
FITC-conjugated mouse anti-CD14	BD Biosciences	Cat# 557153; clone M5E2; RRID:AB_396589
PE-conjugated mouse anti-ASC	BioLegend	Cat# 653903; clone HASC-71; RRID:AB_2564507
<b>Biological samples</b>		
Healthy donor PBMC	This paper	N/A
CMML human PBMC	This paper	N/A
Sepsis human PBMC	This paper	N/A
<b>Chemicals, peptides, and recombinant proteins</b>		
<i>Escherichia coli</i> lipopolysaccharide serotype 0111:B4	InvivoGen	Cat# TLRL-3PELPS
Adenosine 5'-triphosphate	Sigma-Aldrich	Cat# A2383-5G
MCC950	Sigma-Aldrich	Cat# CP-456773
<i>Clostridium difficile</i> toxin B	Enzo Life Sciences	Cat# BML-G150-0050
RPMI 1640 medium	Lonza	Cat# R0883
Fetal bovine serum	Cytiva	Cat# SV30260.03
GlutaMax	Thermo Fisher Scientific	Cat# 35050038
Ficoll Histopaque-1077	Sigma-Aldrich	Cat# 10771
Opti-MEM Reduced Serum Media	Gibco	Cat# 51985-026
DPBS	Thermo Fisher Scientific	Cat# 14200083
IL-1 $\beta$ Human Instant ELISA™ Kit	Invitrogen	Cat# BMS224INST, RRID:AB_2575493
Human IL-18 ELISA Kit	MBL	Cat# 7620, RRID:AB_3065114
IL-18BP Human ELISA kit	Invitrogen	Cat# EHIL18BP
Human TNF-alpha Quantikine ELISA Kit	R&D Systems	Cat# DTA00D, RRID:AB_2941365
Human IL-6 Quantikine ELISA Kit	R&D Systems	Cat# D6050, RRID:AB_2928038
Human P2X purinoceptor 7(P2RX7) ELISA kit	Cusabio	Cat# CSB-EL017325HU
Human HMGB1 ELISA Kit	Arigo Biolaboratories	Cat# ARG81185
Custom MILLIPLEX® kit	Millipore	Cat# HCYTA-60K
Cytotoxicity Detection kit	Sigma-Aldrich	Cat# 11644793001
FACS lysing/fixing solution	BD Biosciences	Cat# 349202
<b>Critical commercial assays</b>		
WES SureSelectXT kit	Agilent Technologies	Cat# G9611C
Maxwell® 16 blood DNA Purification Kit	Promega	Cat# AS1010
<b>Software and algorithms</b>		
GraphPad Prism version 9	GraphPad Software	<a href="https://www.graphpad.com/">https://www.graphpad.com/</a> ; RRID:SCR_002798
Microsoft Excel	Microsoft	<a href="https://www.microsoft.com/en-us/microsoft-365/excel">https://www.microsoft.com/en-us/microsoft-365/excel</a> ; RRID:SCR_016137
ImageJ	FIJI	<a href="https://imagej.nih.gov/ij/">https://imagej.nih.gov/ij/</a> ; RRID:SCR_003070
Gene Expression Omnibus data repository	NCBI Resource	<a href="https://www.ncbi.nlm.nih.gov/geo/">https://www.ncbi.nlm.nih.gov/geo/</a> ; RRID:SCR_005012
SOPHiA DDM platform	SOPHiA Genetics	<a href="https://www.sophiagenetics.com/">https://www.sophiagenetics.com/</a>
TP53 database	National Cancer Institute (NCI)	<a href="https://dceg.cancer.gov/tools/public-data/tp53-database">https://dceg.cancer.gov/tools/public-data/tp53-database</a> ; RRID:SCR_011176
COSMIC database	Sanger Institute	<a href="https://cancer.sanger.ac.uk/cosmic">https://cancer.sanger.ac.uk/cosmic</a>
ClinVar database	National Institutes of Health (NIH)	<a href="https://www.ncbi.nlm.nih.gov/clinvar/">https://www.ncbi.nlm.nih.gov/clinvar/</a>
Milliplex Analyst v.5.2 Flex software	VigenTech	<a href="https://www.vigenetech.com/">https://www.vigenetech.com/</a>
xPONENT® software	Luminex	<a href="https://www.luminexcorp.com/xponent">https://www.luminexcorp.com/xponent</a>

(Continued on next page)

**Continued**

REAGENT or RESOURCE	SOURCE	IDENTIFIER
FCS Express Software	De Novo Software	<a href="https://denovosoftware.com/">https://denovosoftware.com/</a> ; RRID:SCR_016431
CLC Genomics Workbench platform	Qiagen	<a href="https://digitalinsights.qiagen.com/explore/l/clc-gwb-in-trial">https://digitalinsights.qiagen.com/explore/l/clc-gwb-in-trial</a> ; RRID:SCR_017396
BaseSpace	Illumina	<a href="https://developer.basespace.illumina.com/">https://developer.basespace.illumina.com/</a>
DRAGEN Secondary Analysis tool	Illumina	<a href="https://www.illumina.com/products/by-type/informatics-products/dragen-secondary-analysis.html">https://www.illumina.com/products/by-type/informatics-products/dragen-secondary-analysis.html</a>
Galaxy platform	Illumina	<a href="https://usegalaxy.org">https://usegalaxy.org</a>

**Deposited data**

Whole exome sequencing	This paper: Sequence Read Archive (NCBI, <a href="http://www.ncbi.nlm.nih.gov/sra">www.ncbi.nlm.nih.gov/sra</a> )	PRJNA1032543
Raw data	This paper: Zenodo ( <a href="https://zenodo.org">zenodo.org</a> , <a href="https://doi.org/10.5281/zenodo.10074888">https://doi.org/10.5281/zenodo.10074888</a> )	10074888

**Other**

Synergy Mx plate reader	BioTek	N/A
Bio-Plex MAGPIX® multiplex reader	Luminex	40-072
BD Scientific FACSCanto Flow Cytometer	BD Biosciences	RRID:SCR_018055
Maxwell® 16 DNA purification system	Promega	RRID:SCR_020254
MiSeq	Illumina	RRID:SCR_016379
NextSeq 500	Illumina	RRID:SCR_014983
NovaSeq 6000	Illumina	RRID:SCR_016387

**RESOURCE AVAILABILITY**

**Lead contact**

Further information and requests for resources and reagents should be directed to and will be fulfilled by the lead contact, Pablo Pelegrín ([pablo.pelegrin@imib.es](mailto:pablo.pelegrin@imib.es)).

**Materials availability**

This study did not generate new unique reagents.

**Data and code availability**

- The raw sequence data used for analysis is available in NCBI under the Sequence Read Archive (SRA: [www.ncbi.nlm.nih.gov/sra](http://www.ncbi.nlm.nih.gov/sra)) with BioProject No. PRJNA1032543 (see [key resources table](#)). The patient level data reported in this study cannot be deposited in a public repository because of limitations associated with the informed consent. All other original data generated during this study has been deposited at Zenodo ([zenodo.org](https://zenodo.org)) and is publicly available as of the date of publication. DOI is listed in the [key resources table](#).
- This paper does not report original code.
- Any additional information required to reanalyze the data reported in this paper is available from the [lead contact](#) upon request.

**EXPERIMENTAL MODEL AND STUDY PARTICIPANT DETAILS**

**Patients and cohorts**

The clinical-biological characteristics of 19 patients diagnosed with MDS/MPN with mutations in exon 2 or exon 3 of *KRAS* (*KRAS*<sup>mut</sup>) were collected from 7 Spanish highly-specialized hospitals in hematologic molecular diagnosis. Plasma samples at diagnosis from 9 out of the 19 patients were included for this study. Since most of the patients had died or were under hematological treatment, fresh (PB) peripheral blood was available in only 5 patients ([Table S1](#)) who, at the time of the study, were alive and untreated. From one of them, index case ([Table S1](#), patient #1), PB samples were collected at different times. The study also included CMML patients (n = 10) without mutations in exon 2 or 3 of *KRAS* (*KRAS*<sup>wt</sup>), in whom plasma samples (n = 8), and fresh PB (n = 4) were collected ([Table S3](#)).

We used, as controls, healthy individuals ( $n = 9$ ), matched in age and sex with the *KRAS*<sup>mut</sup> patients, and patients with sepsis ( $n = 5$ ). This study was approved by the Clinical Research Ethics Committee of the Hospital Universitario Morales-Meseguer in Murcia, Spain (reference no. 07/19).

### Human clinical samples

CMMML patients' samples were collected from the following hospitals: Hospital General Universitario Morales-Meseguer (Murcia), Hospital Universitario y Politécnico La Fe (Valencia); Hospital Clínico Universitario de Valencia (Valencia), Complejo Universitario de Salamanca (Salamanca), Hospital Universitario 12 de octubre (Madrid), Hospital del Mar, and ICO-Hospital Germans Trias i Pujol (both located in Barcelona). Samples from healthy individuals and patients with sepsis, used as controls, were stored in the Biobank Network of the Region of Murcia [PT13/0010/0018 integrated in the National Biobank Network (B.000859)].

Clinical and demographic characteristics of patients analyzed in this study are provided in [Tables S1](#), [S2](#) and [S3](#). All patients gave informed consent and studies were approved by their respective ethical review committees. Raw sequencing data from patient samples from Hospital General Universitario Morales-Meseguer have been deposited at Sequence Read Archive (SRA) with BioProject No. PRJNA1032543.

## METHOD DETAILS

### Cells and treatments

Whole PB samples were cultured with RPMI 1640 medium (Lonza) containing 10% fetal calf serum (FCS, Cytiva) and 2 mM GlutaMax (Thermo Fisher Scientific). In some experiments, PB mononuclear cells (PBMC) were collected using Ficoll Histopaque-1077 (#10771, Sigma-Aldrich) and 500,000 cells were cultured in 24 well cell culture plate in 500  $\mu$ L of Opti-MEM Reduced Serum Media (#51985-026, Gibco). PB or PBMCs were treated with 1.6  $\mu$ g/mL lipopolysaccharide (LPS) for 2 h at 37°C, and subsequently stimulated with 3 mM adenosine 5'-triphosphate (ATP) for 30 min (to trigger NLRP3 inflammasome activation) or 1  $\mu$ g/mL Clostridium difficile toxin B (TcdB) for 1 h (to trigger Pysin inflammasome activation). In some cases, 10  $\mu$ M MCC950 was added 10 min before ATP or TcdB and maintained during stimulation.

### Evaluation of monocytes with ASC by flow cytometry

For the evaluation of monocytes with ASC by flow cytometry, PB treatment with ATP was for 15 min and TcdB for 30 min. After treatment erythrocytes were lysed under mild hypotonic conditions while preserving and fixing leukocytes with FACS lysing/fixing solution (#349202, BD Biosciences). Monocytes were stained and gated with fluorescein (FITC)-conjugated mouse anti-CD14 monoclonal antibody (clone M5E2; catalog #557153; BD Biosciences, 1:10). The detection of ASC specks in monocytes was done by Time-of-Flight Inflammasome evaluation technique, as we have recently described<sup>24,25</sup> using phycoerythrin (PE)-conjugated mouse anti-ASC monoclonal antibody (HASC-71 clone; #653903; BioLegend, 1:500) and the FACS-Canto flow cytometer (BD Biosciences). Data was analyzed with the FCS Express Software (*De Novo* Software). For gating strategy and representative results see [Figures S2A–S2D](#).

### Lactate dehydrogenase assay

To measure cell death, lactate dehydrogenase (LDH) present in cell-free supernatants was detected using the Cytotoxicity Detection kit (Roche) according to manufacturer instructions, the reaction was read in a Synergy Mx (BioTek) plate reader at 492 nm and corrected at 620 nm.

### Cytokine evaluation

Plasma or cell-free supernatants from fresh EDTA-anticoagulated PB samples from CMMML patients and controls were used to quantify the concentration of human IL-1 $\beta$  (#BMS224INST, Invitrogen), human IL-18 (#7620, MBL), human IL-18BP (#EHIL18BP, Invitrogen), human TNF- $\alpha$  (#DTA00D, R&D Systems), human IL-6 (#D6050, R&D Systems), human ASC (#CSB-EL019114HU, Cusabio), human soluble P2X7 receptor (#CSB-EL017325HU, Cusabio), and human HMGB1 (#ARG81185, Arigo Biolaboratories) by ELISA following the manufacturer's instructions. Results were read on a Synergy Mx plate reader (BioTek) at 450 nm and corrected at 540 nm and 620 nm. Plasma levels of 15 inflammatory cytokines associated with NLRP3-inflammasome, NF- $\kappa$ B and other inflammatory pathways [IL-1 $\alpha$ , IL-1 $\beta$ , IL-1RA, IL-12 (p40 and p70), IL-18, IL-6, IL-8, TNF- $\alpha$ , IL-15, MCP-1/CCL2, M-CSF, GM-CSF, IL-2 and IL-10] were measured using a custom MILLIPLEX kit (#HCYTA-60K, Millipore). A MAGPIX system (Luminex), using xPONENT software, was used for analysis, and the cytokines concentrations were obtained using MilliplexAnalyst v.5.2 Flex software (VigeneTech). GM-CSF, IL-2 and IL-10 were not analyzed as they were not detected in most samples.

### Sequencing analysis

High-throughput sequencing by gene panel (HTS) was performed on diagnostic samples from patients included as CMMML ( $n = 28$ ) or MDS/MPN ( $n = 1$ ). The HTS panel included at least the following 22 genes related to myeloid disorders (ASXL1, CALR, CBL, CSF3R, DNMT3A, ETV6, EZH2, IDH1, IDH2, JAK2, KIT, KRAS, MPL, NRAS, RUNX1, SETBP1, SF3B1, SRSF2, TET2, TP53, U2AF1 and ZRSR2), BioProject PRJNA1032543. Briefly, DNA was extracted from PB or bone marrow (BM) samples and, once the library



was ready, amplified on Illumina platforms (MiSeq and NextSeq 500). Results were analyzed using the SOPHiA DDM platform with its proprietary pipeline or in-house pipelines from Galaxy platform tools (FastQC for quality control, BWA/Bowtie2 for genome alignment and SAMtools for variant calling). Only pathogenic variants with a variant allele frequency (VAF) greater than 2% or more than 10 mutated reads were reported.

### Whole exome sequencing

Whole-exome sequencing was performed by using NovaSeq 6000 (Illumina). Libraries to be sequenced were generated using WES SureSelectXT kit (Agilent Technologies) and the protocol “SureSelectXT Target Enrichment System for Illumina Version B.2, April 2015”. The reads obtained were paired-end (2x150bp), with an average depth per nucleotide of 100 reads, 150 million reads per sample and Phred Quality Score 30 (Q30) >95%, generating a file of between 10 and 15 GB per sample, in a FASTQ format (BioProject PRJNA1032543). Bioinformatics analysis was performed using validated tools from BaseSpace (Illumina). Initial prioritization of both somatic and germline variants was performed using its proprietary pipeline (DRAGEN Somatic or DRAGEN Germline, respectively), and CLC Genomics Workbench (Qiagen) for variant calling, eliminating intronic, synonymous and those with a minor allelic variant greater than or equal to 1%. The final prioritization of germline variants was performed according to the criteria of the American College of Medical Genetics/Association of Molecular Pathologists (ACMG/AMP) and somatic variants were defined as recurrently mutated variants that had been reported by more than one author in the main databases (COSMIC, TP53 Database, ClinVar). Finally, for the index patient, we filtered for genes known to be involved in inflammasome-related diseases ([Table S4](#)).

### QUANTIFICATION AND STATISTICAL ANALYSIS

Statistical analyses were performed using GraphPad Prism version 9 (GraphPad Software Inc.). Continuous variables were presented as mean  $\pm$  SEM or median (interquartile range, IQR), as appropriate, and categorical variables were presented as percentages. Comparisons of categorical variables between groups were performed using the  $\chi^2$  test for tables, while continuous variables were compared using the two-tailed Student's *t* test or the Mann-Whitney U test, as appropriate. Normality of values was determined with the D'Agostino and Pearson omnibus K2 normality test. For comparisons between two groups do not following normality distribution, the two-tailed Mann-Whitney U test was applied, setting the significance level at  $p < 0.05$ . For dataset GSE135902 gene expression comparison, the Wilcoxon signed rank tests with Benjamini–Hochberg correction was used.